

# EVALUATION OF LOW HEAT CONDUCTIVITY RF CABLES\*

G. Cheng<sup>†</sup>, G. Ciovati, M. Morrone, Jefferson Lab, Newport News, VA, USA

## Abstract

New potential applications of superconducting radio-frequency can be envisioned with conduction cooling of the cavities using cryocoolers. In this case, the total heat load to the cryocoolers have to be carefully managed to assure sufficient margin to operate the cavity at an acceptable accelerating gradient. The static and dynamic heat load from rf cables connected to the cavity can be a significant contribution to the total heat load. In this contribution we report the results from measurements of the temperature profile at 1.3 GHz for two low heat conductivity rf cables, as a function of the rf power and with one end of the cable in thermal contact with a liquid helium bath at 4.3 K. A parametric model of the two cables was developed with ANSYS to match the temperature profiles and calculate the heat load at the cold end of the cable.

## INTRODUCTION

Recent developments in Nb<sub>3</sub>Sn films for application to superconducting radio-frequency (SRF) cavities have resulted in quality factor values at 4.3 K and maximum accelerating gradients sufficiently high to be considered for a real accelerator application [1]. In particular, cooling of the SRF cavity using one or multiple cryocooler, instead of a liquid helium bath becomes a feasible option. Such possibility would result in much simplified, cost effective and reliable cryomodules that could be attractive for use in industrial accelerators [2, 3].

As the cooling power of a cryocooler is currently limited to ~2 W at 4 K, careful management of all the heat loads is necessary in order to allow the largest fraction of the total cooling capacity to be available for the cavity rf losses. One source of both static and dynamic heat loads is represented by the rf cables used to transmit power into and out of the cavity. Such cables have one end at room temperature and the other end connected to an rf feedthrough attached to the cold cavity. Ideally, the cables would have low heat conductivity to minimize the static heat load and high electrical conductivity to minimize the dynamic heat load. Such type of cables can be used for the cavity field probe signal and high-order mode coupler signal in traditional cryomodules as well.

In this contribution, we present the results of measurements of the temperature profile and rf losses of two rf cables with one end at room temperature and the other end connected to a flange immersed in liquid helium at 4.3 K. The data have been used to find a suitable parametrization of the thermal model of the cables. The static and dynamic

heat load at different input power levels were then computed from a thermal analysis using ANSYS.

The two semi-rigid, coaxial rf cables with 50 Ω impedance selected for this study are: ULT-05 from KEYCOM, Japan [4], and TFlex-405 from TIMES MICROWAVE SYSTEMS, USA [5].

## RF CABLES SPECIFICATIONS

The ULT-05 cable has an outer conductor made of stainless steel 304 with a 5 μm thick copper plating on the inner surface. The outer diameter (OD) of the outer conductor is 2.2 mm. The dielectric is made of foamed PTFE and has an OD of 1.62 mm. The inner conductor of 0.51 mm diameter is made of silver-plated brass with plating thickness of 3.5 μm. The nominal insertion loss at 1 GHz is 0.9 dB/m at 25 °C. The manufacturer did not provide a maximum power rating but recommended not to exceed 1 W at 1 GHz.

The TFlex-405 cable has a 0.51 mm diameter center conductor made of silver covered copper clad steel. The dielectric, 1.62 mm OD, is made of solid PTFE. It has an inner shield made of silver-plated copper flat ribbon tape and an outer shield, 2.2 mm diameter, made of silver-plated copper braid. The cable also has a blue Teflon FEP jacket. The nominal insertion loss at 1 GHz is 0.69 dB/m at 25 °C. The maximum cw power rating at 1 GHz and 40 °C is 119 W (1:1 VSWR).

## CRYOGENIC TESTS

SMA connectors were soldered to both ends of each cable. The total length, end-to-end, including the connectors is 1930 mm. Seven temperature diodes (DT-470, LakeShore Cryotronics) in an SD-package (3.175 × 1.90 mm<sup>2</sup> footprint) have been attached to the cables' outer conductors at the same fixed locations using GE Varnish and Kapton tape. A picture of one of the sensors attached to the TFlex-405 cable is shown in Fig. 1. For the TFlex-405 cable, the jacket was removed in the areas where the diodes were attached, to allow direct mounting to the outer conductor.

The cable is inserted in a vacuum pipe and connected to SMA feedthroughs on 2.75" Conflat flanges at either end. Four Gore-Tex spacers were used to keep the cable centered in the pipe. The vacuum pipe is part of a test stand to be inserted in a vertical cryostat at Jefferson Lab's Vertical Test Area. A bellow is used at the end section of the pipe to accommodate for the length of the cable and provide some margin for the shrinkage after cooldown. An auxiliary cable (TFlex-402, TIMES MICROWAVE SYSTEMS, USA) is connected to a separate SMA feedthrough on the top plate of the test stand and is used for transmitting the power from the cold end of the cable under test up to room temperature. A picture of the test stand is shown in Fig. 2.

\* Authored by Jefferson Science Associates, LLC under U.S. DOE Contract No. DE-AC05-06OR23177

<sup>†</sup>cheng@jlab.org

Content from this work may be used under the terms of the CC BY 3.0 licence (© 2019). Any distribution of this work must maintain attribution to the author(s), title of the work, publisher, and DOI.

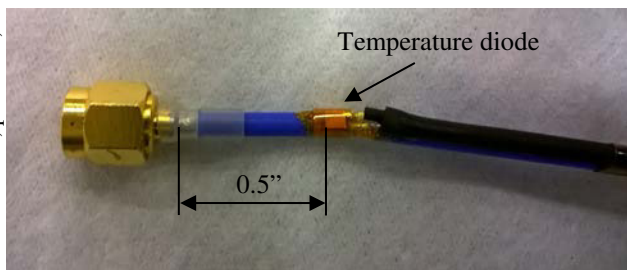


Figure 1: Picture of one end of the TFlex-405 cable with a temperature diode.

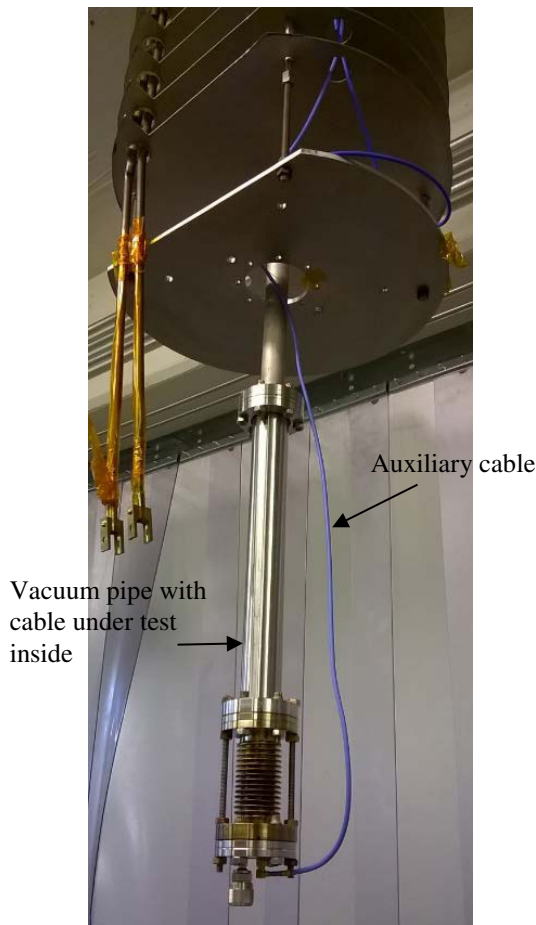


Figure 2: Picture of the test stand with a vacuum pipe and bellow and the auxiliary cable. The rf cable under test is inside the vacuum pipe.

### Insertion Loss

A short-circuit standard was connected at the end of the auxiliary cable and to the SMA feedthrough at the end of the vacuum pipe. A calibrated Cernox resistance-temperature device was attached to the flange at the bottom of the vacuum pipe. The test stand was inserted in a vertical cryostat in Jefferson Lab's Vertical Test Area and the vacuum pipe was evacuated to  $\sim 1 \times 10^{-6}$  mbar. The cryostat was filled with liquid He at 4.3 K, up to the height of the bellow.

A vector network analyser (VNA) (E5071C, Agilent Technologies) was connected using a launching cable firstly to the SMA feedthrough on the top plate to which the cable under test is connected to, and secondly to the

SMA feedthrough on the top plate to which the auxiliary cable is connected to. The VNA was calibrated up to the end of the launching cable. The reflection coefficient  $S_{11}$  was measured over the frequency range 0.5 – 2 GHz and the insertion loss is given by  $|S_{11}|/2$ . The measurements were done both at 300 K and 4.3 K for both the TFlex-405 and the ULT-05 cables and the results are shown in Fig. 3.

The insertion loss per unit length measured at 1 GHz for the TFlex-405 cable, including the SMA connectors and feedthroughs, at 300 K was 0.76 dB/m, whereas it was 1.6 dB/m for the ULT-05 cable. The insertion loss per unit length was significantly higher than the specification for the ULT-05 cable and the presence of a standing-wave pattern with significant amplitude may indicate a possible issue with the cable itself or the connectors soldered to its ends.

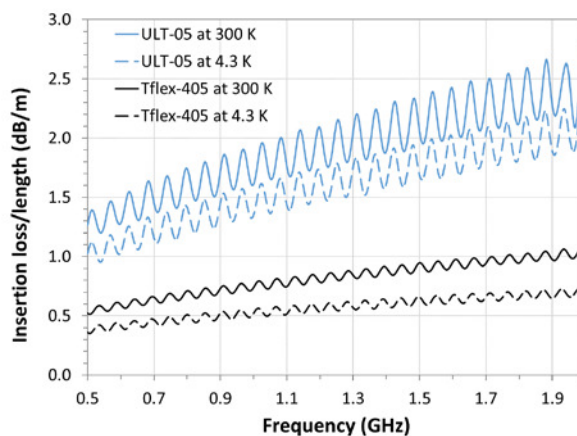


Figure 3: Insertion loss per unit length measured at 300 K and with one end at 4.3 K as a function of frequency for the ULT-05 and the TFlex-405 cables.

### Temperature Profiles

After the measurements of the insertion loss, the test stand was removed from the dewar after warm up, and the auxiliary cable was connected to the SMA feedthrough at the bottom of the vacuum pipe. The cable under test is connected to the vacuum side of the same feedthrough. The stand is inserted back into the dewar, cooled to 4.3 K.

An rf signal generator set at 1.3 GHz drives a high-power amplifier and the output power is measured by a power meter connected to the coupling port of a -30 dB coupler. The rf power is sent into the cable under test through the SMA feedthrough on the test stand top plate. The power flows back up to an SMA feedthrough on the top plate through the auxiliary cable and is dissipated into a 50  $\Omega$  load connected on the air-side of the feedthrough. The power from the auxiliary cable is measured with a power meter connected to the coupling port of another -30 dB coupler between the feedthrough and the load.

The temperature of the seven diodes is measured with a temperature monitor (Model 218, LakeShore Cryotronics) as a function of time, for different levels of rf power injected into the cable under test. The data are acquired for sufficiently long time to approach steady-state conditions.

Fig. 4 shows an example of the temperature,  $T$ , versus time,  $t$ , measured for the TFlex-405 cable.

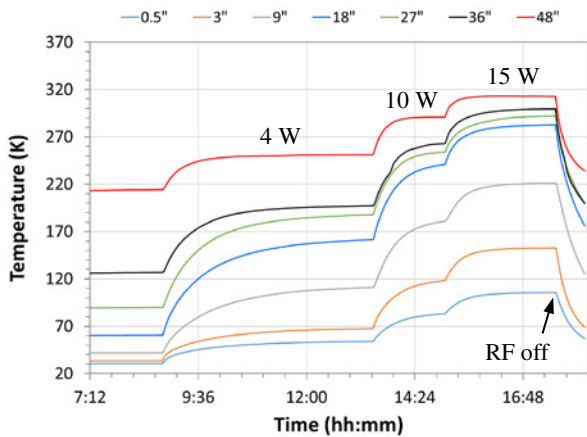


Figure : Temperature versus time measured at several locations from the cold end of the TFlex-405 cable for different levels of input power at 1.3 GHz.

For each power level, the curves of  $T(t)$  were fitted with:

$$T(t) = T_0(1 - e^{-t/\tau}), \quad (1)$$

where  $T_0$  is the steady-state temperature and  $\tau$  is a time constant. Figs. 5 and 6 show the steady-state temperature profiles along the ULT-05 and TFlex-405 cables, respectively, for different values of input power, at 1.3 GHz.

The total insertion loss of the ULT-05 and auxiliary cable increased by  $\sim 0.5$  dB between 0.5 W and 4.4 W, whereas it increased by  $\sim 0.3$  dB between 0.5 W and 15 W for the TFlex-405 and auxiliary cable.

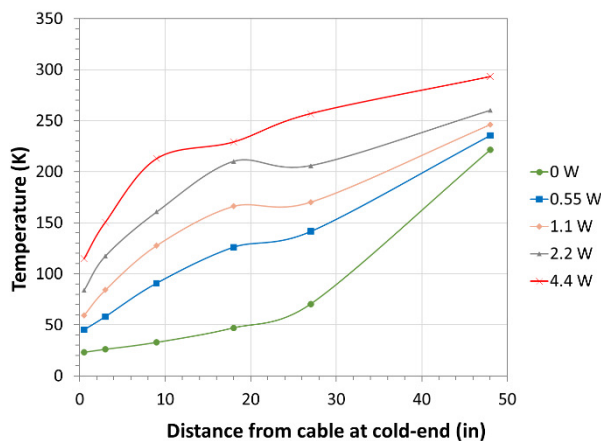


Figure 5: Steady state temperature along the ULT-05 cable for different input power levels at 1.3 GHz.

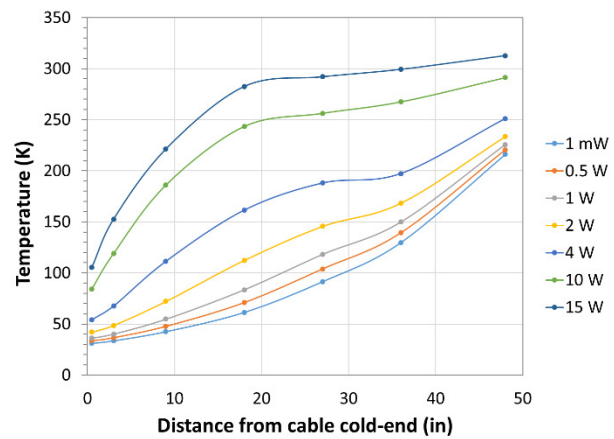


Figure 6: Steady state temperature along the TFlex-405 cable for different input power levels at 1.3 GHz.

## ANSYS SIMULATIONS

Parametric finite element analysis (FEA) models for both the ULT-05 and TFlex-405 cables are created in ANSYS® to simulate their thermal performance with or without RF power. In lieu of constructing a heat load measurement system, FEA models are used to predict the conductive heat to the 4 K boundary and evaluate the benefit of having a 50 K heat station on the RF cable.

The RF cable model consists of the inner conductor, coating for the inner conductor, spacer material between the conductors, the outer conductor and its coating, as well as the external insulation in the case of TFlex-405. Figures 7 and 8 illustrate the cross sections of the ULT-05 and TFlex-405 cables, respectively

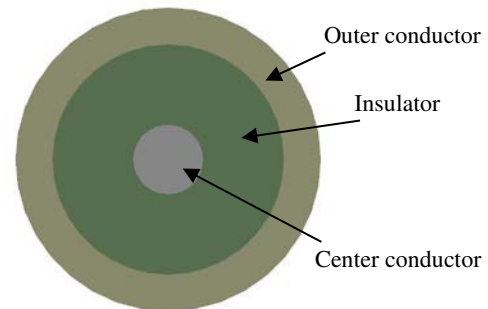


Figure 7: ULT-05 cable model cross section view.

One end of the cable is set to have a temperature boundary of 300 K and the other end is connected to a dummy conductor simulating the SMA connector. The cable model is segmented to have temperature sampling locations matching with those of the temperature sensors used in measurements, i.e. at 0.5", 3", 9", 18", 27", 36" and 48" away from the cold end. Figure 9 illustrates the segmented cable. The dummy conductor's cold end is set to have 4.3 K temperature boundary condition.

Content from this work may be used under the terms of the CC BY 3.0 licence (© 2019). Any distribution of this work must maintain attribution to the author(s), title of the work, publisher, and DOI.

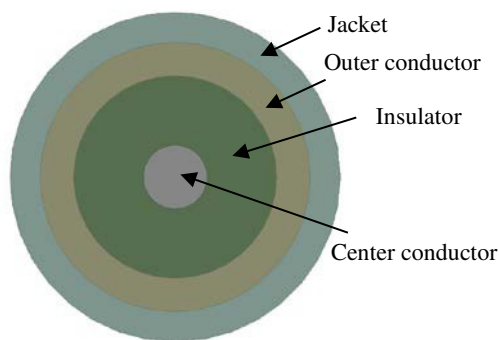


Figure 8: TFLex-405 cable model cross section view.



Figure 9: Segmented TFLex-405 cable model, the cold end dummy conductor locates at the left bottom corner.

The main parameters used to adjust the temperature profile of the cables include the dummy conductor's thermal conductivity, and the conductors' RRR of copper plating, thicknesses of copper/silver coating and thermal emissivities [6]. It is found that the outer conductor's coating thickness has the most significant influence on the temperatures at the sampling points. Temperature dependent thermal conductivities [7] of brass, copper, silver, stainless steel and Teflon are applied to corresponding inner/outer conductors, spacer/insulation and coatings.

Figure 10 shows the comparisons of analysed vs. measured temperatures for both types of RF cables with or without RF power. It is seen that after adjusting the parameters in the model, for the case of zero RF power, both cable models result in temperatures matching the measured data very well. When there is RF power in the cable, the simulated temperatures generally match with the measured data as well. The good agreement between the FEA results and measured data suggests that the models can be adapted to estimate the 4 K heat loads and optimize the 50 K heat station location.

According to the measured loss as shown in Fig. 3, for 1.3 GHz, the cold end losses for the ULT-05 and TFLex-405 are 1.726 dB/m and 0.57 dB/m, respectively. This means that to transmit the same power,  $P_T$ , at the cold end, ULT-05 and TFLex-405 need 4.4 W and 2.59 W input power,  $P_{in}$ , respectively. The power loss,  $P_L$ , is different in the two cables.

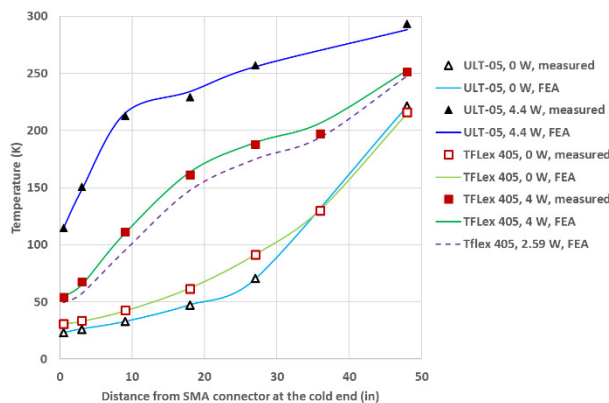


Figure 10: Simulated (FEA) vs. measured temperatures on the ULT-05 and TFLex-405 cables.

50 K heat station optimization is carried out for ULT-05 with  $P_{in} = 4.4$  W and TFLex-405 with 2.59 W, respectively. Figure 11 shows the result of the 50 K heat station location optimization based on the FEA models. In the optimization process, a 50 K boundary condition is applied to the outer conductor of the RF cable. For TFLex-405, in practice that means to peel off the insulation then attach the heat intercept block. As it can be seen from Fig. 11, the TFLex-405 cable results in lower heat load to 4 K than that for the ULT-05 cable, for the same power transmitted at the end of the cable.

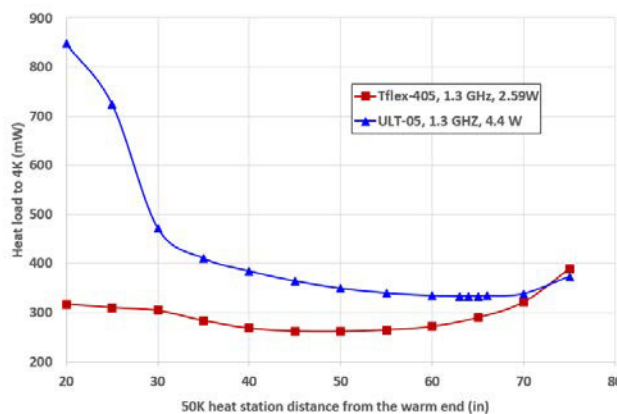


Figure 11: Optimization of 50 K heat station location on ULT-05 and TFLex-405 with 4.4 W and 2.59 W, 1.3 GHz input power, respectively.

Table 1 gives a summary of the input power, cable losses and heat load to 4 K with or without 50 K heat station for both cables. The heat stations are placed at the optimal locations as shown in Fig. 11. A conservative assumption is made that the cable loss in dB/m is not affected by the addition of 50 K heat station. In reality, the 50 K heat station is expected to lower the cable loss.

Table 1: Summary of Input Power, Power Loss, Transmitted Power and Static,  $Q_{S-4K}$ , and Total Heat Loads,  $Q_{4K}$  to 4 K

f = 1.3 GHz	ULT-05		TFlex-405	
	No Heat station	50 K at 63"	No Heat station	50 K at 50"
$P_{in}$ (W)	4.4		2.59	
dB/m	1.73		0.57	
$P_L$ (W)	2.41		0.598	
$P_T$ (W)	1.99		1.99	
$Q_{S-4K}$ (W)	0.013	0.304	0.319	0.226
$Q_{4K}$ (W)	0.982	0.333	0.447	0.261

### CONCLUSION

The experimental and analytical studies of two candidate low loss RF cables, i.e. ULT-05 and TFlex-405, were conducted. The analysis model is parameterized so that good match between the simulated results and measured data can be achieved by fine-tuning the parameters. The tuned cable model is then used to estimate the heat load to 4 K and optimize the location of the 50 K heat station. The TFlex-405 cable is found to have the potential to minimize the 4 K heat load to be around 261 mW at 1.3 GHz and for 2 W RF power transmitted at the cold end.

### ACKNOWLEDGEMENTS

We would like to thank L. King and E. Daly for useful discussions.

### REFERENCES

- [1] S. Posen and D. L. Hall, "Nb<sub>3</sub>Sn superconducting radiofrequency cavities: fabrication, results, properties, and prospects", *Supercond. Sci. Technol.*, vol. 30, p. 033004, 2017. doi:10.1088/1361-6668/30/3/033004
- [2] R. D. Kephart *et al.*, "SRF, Compact Accelerators for Industry & Society", in *Proc. 17th Int. Conf. RF Superconductivity (SRF'15)*, Whistler, Canada, Sep. 2015, paper FRBA03, pp. 1467-1473.
- [3] G. Ciovati *et al.*, "Design of a cw, low-energy, high-power superconducting linac for environmental applications", *Phys. Rev. Accel. Beams*, vol. 21, p. 09160, 2018. doi:10.1103/PhysRevAccelBeams.21.091601
- [4] ULT-05 cable, <http://www.key-com.co.jp/eproducts/upj/upj2/page.htm>
- [5] TFlex-405 cable, <https://www.timesmicrowave.com/DataSheets/Categories/TFlex.pdf>
- [6] J. Frolec, *et al.*, "A database of metallic materials emissivities and absorptivities for cryogenics", *Cryogenics*, vol. 97, pp. 85-99, 2019. doi.org/10.1016/j.cryogenics.2018.12.003
- [7] National Institute of Science & Technology (NIST) material properties: <https://trc.nist.gov/cryogenics/materials/materialproperties.htm>